Journal of Applied Analysis and Computation
Volume 16, Number 6, December 2026, 3320–3336

Website:http://www.jaac-online.com
DOI:10.11948/20250347

NUMERICAL SOLUTIONS OF MULTI-TERM VARIABLE ORDER FRACTIONAL DIFFERENTIAL EQUATION BASED ON LEGENDRE POLYNOMIALS

Bin Xu[1] and Yingchao Zhang[2,†]

Abstract This paper proposes a novel framework for the numerical solution of multi-term variable-order fractional differential equations. By leveraging the properties of Legendre polynomials, we construct an orthonormal basis within a reproducing kernel space, which facilitates the formulation of an efficient $\varepsilon-$approximate solution. The algorithm's robustness is underpinned by a rigorous convergence analysis, and its computational efficiency and high accuracy are further substantiated through three illustrative numerical examples.

Keywords Multi-term constant order fractional differential equation, convergence, Legendre polynomials, $\varepsilon-$approximation solution.

MSC(2010) 65L10, 34A08, 26A33.

1. Introduction

Fractional differential equations (FDEs) are well-suited for simulating physical phenomena and dynamic processes due to their inherent characteristics of memory, heredity, and non-locality, which are particularly relevant in complex environments [7, 31, 33]. In general, it is very tedious to find the exact solutions to fractional differential equations. Therefore, numerical and approximate methods must be employed to approximate the solutions of such equations. In [8], Mehdi proposed approximating the Caputo fractional derivative using sine and cosine functions. Pradip Roul et al. [21–23] developed a high-order numerical technique for the two-dimensional time-fractional equation. A robust adaptive moving mesh technique for a time-fractional reaction?diffusion model was proposed in [20]. Other methods for solving numerical solutions of partial differential equations were proposed in [3, 17, 24, 25].

Fractional linear control systems, often modeled as multi-term constant-order FDEs, can more effectively reveal a system's essential characteristics and achieve enhanced control performance. Moreover, multi-term variable-order FDEs offer even greater modeling potential, enabling more accurate representation of complex dynamic behaviors, especially those involving transient states. To capture such time-varying dynamics, fractional derivatives with time-dependent orders have been introduced, leading to the development of variable-order differential equations [2]. However, similar to their constant-order counterparts, variable-order fractional differential equations often involve multiple terms of variable fractional derivatives, which complicates the derivation of analytical solutions. Therefore, investigating numerical methods for solving multi-term variable-order FDEs is of significant importance. A variety of numerical

[†]The corresponding author.
[1]AVIC General Huanan Aircraft Industry CO., LTD, 519060 Zhuhai, China
[2]Zhuhai College of Science and Technology, 519040 Zhuhai, China
Email: 1170726820@qq.com(B. Xu), zhych0314@163.com(Y. Zhang)

approaches have been proposed to address this challenge, including polynomial methods [5], collocation methods [6], Galerkin finite element methods [12], Lagrange multiplier techniques [18], iterative methods [9], and wavelet methods [26], among others.

In this paper, we consider the multi-term variable-order fractional differential equation (FDEs):

$$\begin{cases} \sum_{k=0}^{m}(a_k(t)D^{\alpha_k(t)}u(t)) + q(t)u(\tau(t)) = f(t), \quad t \in (0,b), \\ u(0) = 0, Bu(b) = \beta, \end{cases} \tag{1.1}$$

where $D^{\alpha_k(t)}u(t)$ $(k = 0, 1, 2, \cdots, m)$ is the fractional derivatives in the Caputo sense and $\alpha_k(t) \in [0, 2]$. $a_k(t)$, $q(t)$ and $\tau(t)$ are all continuous function on $[0, b]$. $B : W_2[0, b] \to R$ is a linear functional.

In recent years, reproducing kernel methods have been widely adopted by researchers for obtaining numerical solutions to both classical differential equations [28, 29] and fractional differential equations [34]. For instance, Zhang, Zheng et al. constructed sets of orthogonal bases in reproducing kernel spaces and developed corresponding numerical schemes for boundary value problems of differential equations [36–38]. They also provided theoretical analyses regarding the feasibility, convergence order, and stability of these methods. Inspired by the least squares method, Xu et al. proposed effective algorithms for solving fractional integro-differential equations [11] and interface problems [30]. Since multi-term fractional differential equations involve multiple fractional-order derivative terms, their numerical solution is generally more challenging. Notably, orthogonal bases constructed in reproducing kernel spaces based on Legendre polynomials have demonstrated promising performance in addressing such equations [32, 35]. Lotfi [16] presented the numerical solution of a class of fractional optimal control problems using Legendre polynomials. Building on these developments, this paper employs Legendre polynomials to construct a basis within the reproducing kernel space and incorporates ideas derived from the least squares method to numerically solve multi-term fractional differential equations. The proposed method offers several distinct advantages. The use of an orthonormal basis ensures numerical stability and leads to well-conditioned discrete systems. It achieves spectral accuracy for smooth solutions, exhibiting exponential convergence as the number of basis functions increases. The approach directly handles multi-term and variable-order fractional derivatives without the need for special treatment. Additionally, the least squares framework naturally incorporates boundary conditions, resulting in high-precision approximate solutions.

The remainder of this paper is organized as follows. Section 2 begins by reviewing the definition of the Caputo fractional derivative and then presents Legendre polynomials and their relevant function spaces. The notion of an ϵ-approximate solution is defined in Section 3. Subsequently, a rigorous convergence analysis for the proposed method is established in Section 4. To validate the method's efficacy, Section 5 provides three illustrative numerical examples. The paper concludes with a summary of findings in the final section.

2. Preliminaries

2.1. Caputo fractional calculus

In this section, we first introduce the definitions of Caputo fractional derivatives and the properties to be used in this paper.

Definition 2.1 ([15]). The α order Caputo derivatives of the function $u(t)$ on [0,b] is defined by

$$D^{\alpha}u(t) = \frac{1}{\Gamma(n-\alpha)}\int_0^t (t-x)^{n-1-\alpha}u^{(n)}(x)dx,$$

where $n = [\alpha] + 1$.

Definition 2.2 ([13]). The $\alpha(t)$ order Caputo derivatives of the function $u(t)$ on [0,b] is defined by

$$D^{\alpha(t)}u(t) = \frac{1}{\Gamma(n-\alpha(t))}\int_0^t (t-x)^{n-1-\alpha(t)}u^{(n)}(x)dx,$$

where $n = [\max_{t\in(0,b)} \alpha(t)] + 1$.

Also, when $\alpha(t)$ is an integer, the Caputo derivative is defined the same as the integral derivative of the function $u(t)$. According to Definition 2.2, we can deduce the following properties.

Property 2.1.

$$D^{\alpha(t)}(t^p) = \begin{cases} \dfrac{\Gamma(p+1)}{\Gamma(p+1-\alpha(t))}t^{p-\alpha(t)}, & p \neq 0, \\ 0, & p = 0. \end{cases} \tag{2.1}$$

Property 2.2 ([13]). The dissipative properties of variable-order fractional derivatives:

$$\int_0^b D^{\alpha(t)}u(t)u'(t))dt \geq \|u'\|_{L^2}^2 - C_1\|u\|_{L^2}\|u'\|_{L^2}.$$

Where C_1 is a constant.

2.2. Legendre polynomials and related space

This section introduces Legendre polynomials and reproducing kernel spaces. According to Legendre polynomials, a set of orthonormal bases is constructed in this section.

Definition 2.3 ([27,38]). $W_2[0,b] = \{u(t) \mid u(0) = u'(0) = 0,\ u \text{ is absolutely continuous}, u'' \in L^2[0,b]\}$, and

$$\langle u, v\rangle_{W_2} = \int_0^b u''v''dt, \qquad u, v \in W_2[0,b].$$

It is well known that Legendre polynomials are orthogonal on $L^2[-1,1]$. To facilitate the study of the problem, we extend them to the interval $[a,b]$ via an appropriate change of variables. The resulting shifted Legendre polynomials on $[a,b]$ are defined as follows.

$$l_0(t) = 1, \quad l_1(t) = \frac{2(t-a)}{b-a} - 1,$$
$$l_{j+1}(t) = \frac{2j+1}{j+1}[\frac{2(t-a)}{b-a} - 1]l_j(t) - \frac{j}{j+1}l_{j-1}(t), \quad j = 1, 2, \cdots.$$

The orthogonality of $\{l_j(t)\}_{j=0}^{\infty}$ on $L^2[a,b]$ is obvious, and

$$\int_a^b l_i(t)l_j(t)dt = \begin{cases} \dfrac{b-a}{2j+1}, & i = j, \\ 0, & i \neq j. \end{cases}$$

Let $a=0$ and a set of orthonormal basis $p_j(t)=\sqrt{\frac{2j+1}{b}}l_j(t)$ on $L^2[0,b]$ is obtained. Next, we use $p_j(t)$ to construct the basis functions on $W_2[0,b]$.

Note $p_j(t)=\sum_{k=0}^{j}c_kt^k$, then

$$J_0^2p_j(t)=\int_0^t\int_0^s p_j(x)dxds=\sum_{k=0}^{j}c_k\frac{t^{k+2}}{(k+1)(k+2)}.$$

Theorem 2.1. *$\{J_0^2p_j(t)\}_{j=0}^{\infty}$ is a set of orthonormal basis on $W_2[0,b]$.*

Proof. Only need to prove completeness and orthogonality. Because

$$\langle J_0^2p_i(t),J_0^2p_j(t)\rangle_{W_2}=\langle p_i(t),p_j(t)\rangle_{L^2}=\begin{cases}1, & i=j,\\ 0, & i\neq j.\end{cases}$$

Orthogonality is obviously.

Completeness. For $u\in W_2[0,b]$, if

$$\langle u,J_0^2p_j\rangle_{W_2}=0,$$

it can deduce $u\equiv 0$, then $\{J_0^2p_j(t)\}_{j=0}^{\infty}$ are complete. In fact,

$$\langle u,J_0^2p_j\rangle_{W_2}=\langle u'',p_j\rangle_{L^2}=0.$$

Because $p_j(t)=\sqrt{\frac{2j+1}{b}}l_j(t)$ is a set of orthonormal basis on $L^2[0,b]$, $u''\equiv 0$. Due to $u\in W_2[0,b],u(0)=u'(0)=0$, then $u\equiv 0$. □

3. $\varepsilon-$approximate solution

Let $L:W_2[0,b])\to L^2[0,b]$,

$$Lu=\sum_{k=0}^{m}(a_k(t)D^{\alpha_k(t)}u(t))+q(t)u(\tau(t)).$$

Then Eq. (1.1) is

$$Lu=f. \tag{3.1}$$

3.1. The reversibility of L

Theorem 3.1. *$L:W_2[0,b])\to L^2[0,b]$ is a bounded and linear operator.*

Proof. The linearity is obvious, so one only needs to prove boundedness. We know

$$\begin{aligned}\|Lu\|_{L^2}&\leq\|\sum_{k=0}^{m}(a_k(t)D^{\alpha_k(t)}u(t))\|_{L^2}+\|q(t)u(\tau(t))\|_{L^2}\\&\leq\sum_{k=0}^{m}\|a_k(t)D^{\alpha_k(t)}u(t)\|_{L^2}+\|q(t)u(\tau(t))\|_{L^2}.\end{aligned}$$

Let $K_t(x)$ be the reproducing kernel in $W_2[0,b]$. From Ref. [27], by the reproducing property, we obtain

$$|u^{(i)}(t)| = \left|\langle u, \frac{\partial^i K_t}{\partial t^i}\rangle_{W_2}\right| \le \left\|\frac{\partial^i K_t}{\partial t^i}\right\|_{W_2}\|u\|_{W_2},\ i=0,1,2. \tag{3.2}$$

Then there exist positive constant M_0 such that

$$\begin{aligned}\|q(t)u(\tau(t))\|_{L^2} &= \Big(\int_0^b (q(t)u(\tau(t)))^2 dt\Big)^{\frac{1}{2}}\\ &\le \max_{t\in[0,b]}|q(t)|\Big(\int_0^b (u(\tau(t)))^2 dt\Big)^{\frac{1}{2}}\\ &\le \max_{t\in[0,b]}|q(t)|b^{\frac{1}{2}}\|K_t\|_{W_2}\|u\|_{W_2}\\ &= M_0\|u\|_{W_2}.\end{aligned} \tag{3.3}$$

By the definition of Caputo derivatives, there exist positive constant M_k $(k=0,1,2,\cdots)$ such that

$$\begin{aligned}|D^{\alpha_k(t)}u(t)| &= \Big|\frac{1}{\Gamma(n_k-\alpha_k(t))}\int_0^t (t-x)^{n_k-1-\alpha_k(t)}u^{(n_k)}(x)dx\Big|\\ &\le \frac{1}{\Gamma(n_k-\alpha_k(t))}\int_0^t |(t-x)^{n_k-1-\alpha_k(t)}||u^{(n_k)}(x)|dx\\ &\le \frac{\|\frac{\partial^{n_k}K_t}{\partial t^{n_k}}\|_{W_2}\|u\|_{W_2}}{\Gamma(n_k-\alpha_k(t))}\int_0^t |(t-x)^{n_k-1-\alpha_k(t)}|dx\\ &\le \frac{\|\frac{\partial^{n_k}K_t}{\partial t^{n_k}}\|_{W_2}\|u\|_{W_2}}{\Gamma(n_k-\alpha_k(t))}\frac{t^{n_k-\alpha_k(t)}}{n_k-\alpha_k(t)}\\ &\le \frac{\|\frac{\partial^{n_k}K_t}{\partial t^{n_k}}\|_{W_2}\|u\|_{W_2}}{\Gamma(n_k-\alpha_k(t))}\frac{b^{n_k-\alpha_k(t)}}{n_k-\alpha_k(t)}\\ &= M_k\|u\|_{W_2},\end{aligned}$$

where $n_k = [\max\limits_{t\in(0,b)}\alpha_k(t)]+1$. Due to $a_k(t)\in C[0,b]$, then

$$\begin{aligned}\|a_k(t)D^{\alpha_k(t)}u(t)\|_{L^2} &= \left(\int_0^b (a_k(t)D^{\alpha_k(t)}u(t))^2 dt\right)^{\frac{1}{2}}\\ &\le \max_{t\in(0,b)}|a_k(t)|\left(\int_0^b (D^{\alpha_k(t)}u(t))^2 dt\right)^{\frac{1}{2}}\\ &\le b^{\frac{1}{2}}\max_{t\in(0,b)}|a_k(t)|M_k\|u\|_{W_2}.\end{aligned} \tag{3.4}$$

Let $M_2 = \sum\limits_{k=0}^{m}(\max\limits_{t\in(0,b)}|a_k(t)|M_k)$. From Eq. (3.3) and Eq. (3.4), we can get

$$\begin{aligned}\|Lu\|_{L^2} &\le \sum_{k=0}^{m}(b^{\frac{1}{2}}\max_{t\in(0,b)}|a_k(t)|M_k\|u\|_{W_2}) + M_0\|u\|_{W_2}\\ &\le bM_2\|u\|_{W_2} + M_0\|u\|_{W_2} \le M_3\|u\|_{W_2},\end{aligned}$$

where $M_3 = bM_2 + M_0$. $\square$

Theorem 3.2. *L is invertible, and its inverse operator L^{-1} is bounded.*

Proof. According to Eq. (1.1), $a_k(t), q(t) \in C[0,b]$, then $a_k(t), q(t)$ is bounded on $[0,b]$. That is, there exists a constant $\gamma > 0, \delta > 0$, such that $a_k(t) > \gamma$ and $|q(t)| < \delta$.

From Theorem 3.1, L is bounded. By the inverse operator theorem, to prove that L is invertible, it suffices to show that L is one-to-one mapping. That is, if $Lu = 0$, then $u \equiv 0$.

According to Definition 2.2,

$$|D^{\alpha_k(t)}u(t)| = \Big|\frac{1}{\Gamma(n_k - \alpha_k(t))}\int_0^t (t-x)^{n_k-1-\alpha_k(t)}u^{(n_k)}(x)dx\Big|.$$

Due to $\alpha_k \in [0,2]$, $n_k = 1,2$. For simplicity, let $n_k = 1$. Then

$$|D^{\alpha_k(t)}u(t)| = \Big|\frac{1}{\Gamma(1 - \alpha_k(t))}\int_0^t (t-x)^{-\alpha_k(t)}u'(x)dx\Big|.$$

Multiplying both sides of $Lu = 0$ by u' and integrating over [0, b] yields

$$\sum_{k=0}^{m}\int_0^b (a_k(t)D^{\alpha_k(t)}u(t)u'(t))dt + \int_0^b q(t)u(\tau(t))u'(t)dt.$$

For the first term, using the Property 2.2, there exists a constant C_1 such that

$$\int_0^b (a_k(t)D^{\alpha_k(t)}u(t)u'(t))dt \geq \gamma\|u'\|_{L^2}^2 - C_1\|u\|_{L^2}\|u'\|_{L^2}.$$

For the second term, using the Cauchy-Schwarz inequality and $\tau(t) \in C[0,b]$, there exists a constant $\delta > 0$ such that

$$\Big|\int_0^b q(t)u(\tau(t))u'(t)dt\Big| \leq \delta\|u\|_{L^2}\|u'\|_{L^2}.$$

Therefore,

$$\gamma\|u'\|_{L^2}^2 \leq (C_1 + \delta)\|u\|_{L^2}\|u'\|_{L^2}. \tag{3.5}$$

In Eq. (3.5), if $\|u'\|_{L^2} = 0$, it follows from the boundary condition $u = 0$, that $u \equiv 0$. Otherwise, if $\|u'\|_{L^2} \neq 0$, the Poincare inequality gives $\|u\|_{L^2} \leq C_F\|u'\|_{L^2}$, and Eq. (3.5) implied

$$\gamma\|u'\|_{L^2} \leq (C_1 + \delta)\|u\|_{L^2} \leq (C_1 + \delta)C_F\|u'\|_{L^2}.$$

Since C_1, δ, γ and C_F are all constants, if the above expression holds identically, then $\|u'\|_{L^2} = 0$, and consequently $u \equiv 0$.

In summary, L is one-to-one mapping. The theorem is proved. □

3.2. $\varepsilon-$approximate solution

Definition 3.1. For any $\varepsilon > 0$, if

$$\|Lu^\varepsilon(t) - f(t)\|_{L^2}^2 + |Bu^\varepsilon(t) - \beta|^2 < \varepsilon^2.$$

Then $u^\varepsilon(t)$ is called $\varepsilon-$approximate solution to Eq. (3.1).

The existence of $u^\varepsilon(t)$ for the boundary value problems of integer-order differential equations has been established in Refs. [34, 36–38]. By extending the methods from these references, we now present the following theorem concerning the existence of the ε-approximate solution for Eq. (3.1).

Theorem 3.3. *$\forall\ \varepsilon > 0$, $\exists\ N > 0$, when $n > N$,*

$$u_n^\varepsilon = \sum_{i=0}^{n} d_i^* J_0^2 p_i(t)$$

is the $\varepsilon-$approximate solution of Eq. (3.1), *where d_i^* satisfies*

$$\begin{aligned}&\|\sum_{i=0}^{n} d_i^* L(J_0^2 p_i) - f\|_{L^2}^2 + |\sum_{i=0}^{n} d_i^* B(J_0^2 p_i) - \beta|^2\\ &= \min_{d_i}\{\|\sum_{i=0}^{n} d_i L(J_0^2 p_i) - f\|_{L^2}^2 + |\sum_{i=0}^{n} d_i B(J_0^2 p_i) - \beta|^2\}.\end{aligned}$$

Because $L(J_0^2 p_i)$ contains Caputo differential $D^{\alpha_k(t)} J_0^2 p_i$, by Eq. (2.1), you can get

$$\begin{aligned}L(J_0^2 p_i) &= \sum_{k=0}^{m} a_k(t) D^{\alpha_k(t)} J_0^2 p_i(t) + q(t) J_0^2 p_i(\tau(t))\\ &= \sum_{k=0}^{m} a_k(t) D^{\alpha_k(t)} \Big(\sum_{j=0}^{i} \frac{c_j t^{j+2}}{(j+1)(j+2)}\Big) + q(t) J_0^2 p_i(\tau(t))\\ &= \sum_{k=0}^{m} a_k(t) \sum_{j=0}^{i} \frac{c_j D^{\alpha_k(t)} t^{j+2}}{(j+1)(j+2)} + q(t) J_0^2 p_i(\tau(t))\\ &= \sum_{k=0}^{m} \sum_{j=0}^{i} \frac{a_k(t) c_j \Gamma(j+3) t^{j+2-\alpha_k(t)}}{(j+1)(j+2)\Gamma(j+3-\alpha_k(t))} + q(t) J_0^2 p_i(\tau(t)).\end{aligned}$$

From Theorem 3.3, note

$$G(d_0, d_1, d_2, \cdots, d_n) = \|\sum_{i=0}^{n} d_i L(J_0^2 p_i) - f\|_{L^2}^2 + |\sum_{i=0}^{n} d_i B(J_0^2 p_i) - \beta|^2,$$

G is quadratic form with respect to $d = (d_0, d_1, \cdots, d_n)$. Only need to find the minimum value $d^* = (d_0^*, d_1^*, \cdots, d_n^*)$, that is, just need $\frac{\partial G}{\partial d_i} = 0$. We know

$$\frac{\partial G}{\partial d_i} = 2\sum_{j=0}^{n} d_i \langle L(J_0^2 p_i), L(J_0^2 p_j)\rangle_{L^2} - 2d_i \langle L(J_0^2 p_i), f\rangle_{L^2} - 2\sum_{j=0}^{n} d_i B(J_0^2 p_i) B(J_0^2 p_j) - 2B(J_0^2 p_i)\beta.$$

So

$$\sum_{j=0}^{n} d_i \langle L(J_0^2 p_i), L(J_0^2 p_j)\rangle_{L^2} + \sum_{j=0}^{n} d_i B(J_0^2 p_i) B(J_0^2 p_j) = \langle L(J_0^2 p_i), f\rangle_{L^2} + B(J_0^2 p_i)\beta. \tag{3.6}$$

Put

$$\mathbf{A} = \left(\langle L(J_0^2 p_i), L(J_0^2 p_j)\rangle_{L^2} + B(J_0^2 p_i)B(J_0^2 p_j)\right)_{(n+1)\times(n+1)},$$
$$\mathbf{b} = \left(\langle L(J_0^2 p_i), f\rangle_{L^2} + B(J_0^2 p_i)\beta\right)_{(n+1)}.$$

Clearly, both matrix $\mathbf{A}$ and vector $\mathbf{b}$ are of order $n+1$. So Eq. (3.6) is

$$\mathbf{A}d = \mathbf{b}. \tag{3.7}$$

By Theorem 3.2, L is an invertible operator. According to the method introduced in Ref. [34], it can be inferred that Eq. (3.7) has a unique solution.

4. Convergence

4.1. Analysis of convergence

Theorem 4.1. Assume $u(t)$ is the exact solution of Eq. (3.1), $u_n^\varepsilon(t)$ is the $\varepsilon-$approximate solution of Eq. (3.1). Then $u_n^\varepsilon(t)$ uniformly converges to $u(t)$.

Proof. According to Definition 3.1

$$\begin{aligned}\|u(t)-u_n^\varepsilon(t)\|_{W_2}^2 &\le \|L^{-1}\|^2\|L(u-u_n^\varepsilon)\|_{L^2}^2\\ &\le \|L^{-1}\|^2(\|L(u-u_n^\varepsilon)\|_{L^2}^2 + |\beta - Bu_n^\varepsilon|^2)\\ &\le \|L^{-1}\|^2(\|L(u-u_n^\varepsilon)\|_{L^2}^2 + |Bu - Bu_n^\varepsilon|^2)\\ &\le \|L^{-1}\|^2\varepsilon^2.\end{aligned}$$

Suppose $K_t(y)$ is the reproducing kernel of $W_2[0,b]$. From Eq. (3.2), for $\forall u(t)\in W_2[0,b]$,

$$|u(t)-u_n^\varepsilon(t)| = |\langle u(y)-u_n^\varepsilon(y), K_t(y)\rangle_{W_2}| \le \|u(t)-u_n^\varepsilon(t)\|_{W_2}\|K_t\|_{W_2} \le M\varepsilon,$$

where $M = \|K_t\|_{W_2}\|L^{-1}\|^2$.

So $|u(t)-u_n^\varepsilon(t)| \to 0$. □

If

$$u(t) = \sum_{i=0}^{\infty} d_i J_a^2 p_i(t),$$

is the exact solution of Eq. (3.1), and $u_n(t)$ is Fourier truncation of $u(t)$, then

$$u_n(t) = \sum_{i=0}^{n} d_i J_0^2 p_i(t) = \sum_{i=0}^{n}\langle u, J_0^2 p_i(t)\rangle_{L^2} J_0^2 p_i(t).$$

From Ref. [1], if $u^{(m)}(t)\in L^2[0,b]$, then

$$\|u(t)-u_n(t)\|_{L^2} \le Cn^{-m}\left(\sum_{k=\min\{m,n+1\}}^{m}\|u^{(k)}(t)\|_{L^2}^2\right)^{\frac{1}{2}}. \tag{4.1}$$

To discuss the convergence order, the linear functional B needs to be bounded. Since the linear functionals in this paper consist of function values or derivative values, they are clearly bounded according to Eq. (3.2). That is, $|Bu| \le \|B\|\|u\|_{W_2}$.

Theorem 4.2. *Suppose $u(t)$ is the exact solution of Eq.* (3.1), *$u_n^\varepsilon(t)$ is the $\varepsilon-$approximate solution of Eq.* (3.1). *If $u^{(m)}(t) \in W_2[0,b]$, then*

$$\|u(t) - u_n^\varepsilon(t)\|_{W_2} \le Mn^{-m} \left(\sum_{k=\min\{m,n+1\}}^{m} \|u^{(k+2)}(t)\|_{L^2}^2 \right)^{\frac{1}{2}}.$$

Proof. According to Theorem 3.1 and Eq. (4.1)

$$\begin{aligned}
\|u(t) - u_n^\varepsilon(t)\|_{W_2}^2 &\le \|L^{-1}\|^2 (\|L(u - u_n^\varepsilon)\|_{L^2}^2 + |Bu - Bu_n^\varepsilon|^2) \\
&\le \|L^{-1}\|^2 (\|L(u - u_n)\|_{L^2}^2 + |Bu - Bu_n|^2 \\
&\le \|L^{-1}\|^2 (\|L\|^2 \|u - u_n\|_{L^2}^2 + \|B\| \|u - u_n\|_{W_2}^2) \\
&\le (\|L^{-1}(\|L\|^2 + \|B\|^2)\|) \|u - u_n\|_{W_2}^2.
\end{aligned}$$

Obviously, $\|u(t) - u_n^\varepsilon(t)\|_{W_2} \le M_0 \|u(t) - u_n(t)\|_{W_2}$.

Since $u^{(m)}(t) \in W_2[0,b]$, in other words, $u^{(m+2)}(t) \in L^2[0,b]$, that is,

$$\|u(t) - u_n(t)\|_{W_2} = \|u''(t) - u_n''(t)\|_{L^2} = \|u''(t) - \sum_{i=0}^{n} \langle u''(t), p_i(t) \rangle_{L^2} p_i(t)\|_{L^2}.$$

According to Eq. (4.1),

$$\|u(t) - u_n^\varepsilon(t)\|_{W_2} \le M_0 \|u(t) - u_n(t)\|_{W_2} \le Mn^{-m} \left(\sum_{k=\min\{m,n+1\}}^{m} \|u^{(k+2)}(t)\|_{L^2}^2 \right)^{\frac{1}{2}},$$

where M is a constant. □

4.2. Analysis of stability

Analysis of stability is conducted below. According to the third section, the stability of the algorithm is related to the stability of Eq. (3.7). Therefore, the stability of the algorithm can be discussed by the eigenvalues of the matrix **A**. In this paper,

$$\mathbf{A} = (a_{ij}) = \left(\langle L(J_0^2 p_i), L(J_0^2 p_j) \rangle_{L^2} + B(J_0^2 p_i) B(J_0^2 p_j) \right)_{(n+1)\times(n+1)}.$$

Theorem 4.3. *Assume $u \in W_2[0,b]$ and $\|u\|_{W_2} = 1$. Then $\|Lu\|_{L^2} \ge \frac{1}{\|L^{-1}\|}$.*

Proof. From Theorem 3.2, L is an invertible operator. Its inverse operator is L^{-1}. We have

$$1 = \|u\|_{W_2} = \|L^{-1}Lu\|_{W_2} \le \|L^{-1}\| \|Lu\|_{L^2}.$$

Moreover,

$$\|Lu\|_{L^2} \ge \frac{1}{\|L^{-1}\|}.$$

□

Theorem 4.4. *Let λ be the eigenvalue of matrix **A** of Eq.* (3.7). *There exists a constant $C > 0$ satisfy $\lambda > C > 0$. Therefore, Eq.* (3.7) *is stable. That is,*

$$\|d - \tilde{d}\|_2 \le \frac{1}{\lambda((A))} \|\delta b\|_2 \le \|L^{-1}\| \|\delta b\|_2.$$

Proof. Because λ be the eigenvalue of matrix $\mathbf{A}$, let $x = (x_1, \cdots, x_{n+1})^T$ is related eigenvector of λ and $\|x\| = 1$. Then $\mathbf{A}x$=λx,

$$\begin{aligned}\lambda x_i =& \sum_{j=1}^{n+1} a_{ij}x_j\\ =& \sum_{j=1}^{n+1} \left(\langle L(J_0^2 p_i), L(J_0^2 p_j)\rangle_{L^2} + B(J_0^2 p_i)B(J_0^2 p_j)\right) x_j\\ =&\langle L(J_0^2 p_i), \sum_{j=1}^{n+1} x_j L(J_0^2 p_j)\rangle + B(J_0^2 p_i)\sum_{j=1}^{n+1} B(J_0^2 p_j))x_j.\end{aligned}$$

Let x_i multiply to bothsides of equation, then add the equations from $j = 1$ to $n + 1$ so that

$$\begin{aligned}\lambda =& \lambda x_i^2\\ =& \Big\langle \sum_{i=1}^{n+1} x_i L(J_0^2 p_i), \sum_{j=1}^{n+1} x_j L(J_0^2 p_j)\Big\rangle + \Big(\sum_{j=1}^{n+1} B(J_0^2 p_j))x_j\Big)^2\\ =& \Big\|\sum_{i=1}^{n+1} x_i L(J_0^2 p_i)\Big\|_{L^2}^2 + \Big(\sum_{j=1}^{n+1} B(J_0^2 p_j))x_j\Big)^2\\ \geq& \Big\|\sum_{i=1}^{n+1} x_i L(J_0^2 p_i)\Big\|_{L^2}^2.\end{aligned}$$

From Theorems 2.1 and 4.3, we can get

$$\lambda \geq \Big\|\sum_{i=1}^{n+1} x_i L(J_0^2 p_i)\Big\|_{L^2}^2 = \Big\|L\Big(\sum_{i=1}^{n+1} x_i J_0^2 p_i\Big)\Big\|_{L^2}^2 \geq \frac{1}{\|L^{-1}\|}.$$

Assume d and $\tilde{d}$ satisfy

$$\mathbf{A}d = b, \qquad \mathbf{A}\tilde{d} = b + \delta b.$$

Subtracting, we get $A(\tilde{d} - d) = \delta b$,

$$\|\tilde{d} - d\|_2 = \|\mathbf{A}^{-1}\delta b\|_2 \leq \|\mathbf{A}^{-1}\|_2\|\delta b\|_2 = \frac{1}{\lambda_{\min}(A)}\|\delta b\|_2 \leq \|L^{-1}\|\|\delta b\|_2,$$

where $\|(A)^{-1}\|_2 = \frac{1}{\lambda_{\min}(A)}$ is spectral norm. □

5. Numerical examples

This section presents numerical examples to illustrate the effectiveness and convergence of the proposed method. The number of basis functions used is denoted by n. We define the absolute error as $e_n(t) = |u(t) - u_n(t)|$ and the maximum absolute error as ME_n. The numerical results, compared with those from Refs. [4, 10, 14, 19], are summarized in 8 tables and 8 figures. These results demonstrate that the method presented in this paper is highly effective.

Example 5.1. Consider the first test problem suggested in Refs. [10, 14]

$$\begin{cases} D^{\alpha(t)}u(t) + \cos t u'(t) + 4u(t) + 5u(t^2) = f(t), \quad t \in (0,1), \\ u(0) = 0, u(1) = 1, \end{cases}$$

where the exact solution is $u(t) = t^2$, $f(t) = \frac{2t^{2-\alpha(t)}}{\Gamma(3-\alpha(t))} + 5t^4 + 4t^2 + 2t\cos t$, and $\alpha(t) = \frac{5+\sin t}{4}$. The numerical results are summarized in Tables 1 and 2. Table 1 demonstrates that the solutions generated by the presented method converge at various points, highlighting its superiority over the method in Refs. [10, 14]. Furthermore, Table 2 lists the corresponding maximum absolute errors and CPU for Example 5.1 when $\alpha(t)$ is a constant.

Table 1. $e_n(t)$ of Example 5.1.

t	[14]	[10]	our method
0.1	1.43e–6	1.17e–8	8.73e–18
0.2	2.28e–6	1.77e–8	7.67e–17
0.3	2.84e–6	2.17e–8	2.24e–16
0.4	3.11e–6	2.39e–8	4.31e–16
0.5	3.13e–6	2.45e–8	6.55e–16
0.6	2.94e–6	2.34e–8	8.53e–16
0.7	2.53e–6	2.07e–8	1.00e–15
0.8	1.88e–6	1.59e–8	1.10e–15
0.9	9.97e–7	1.11e–8	1.25e–15

Table 2. ME_4 of Example 5.1.

t	$\alpha(t) = 1.2$	$\alpha(t) = 1.5$	$\alpha(t) = 1.9$
ME_4	3.28e-15	1.72e-15	1.25e-16
CPU	0.25	0.25	0.25

Example 5.2. Consider the second test problem which models the general damped mechanical oscillator in Refs. [4, 19]:

$$\begin{cases} D^{\alpha(t)}u(t) + qD_0^{\beta(t)}u(t) + ru(t) = f(t), \quad t \in (0,1), \\ u(a) = 0, u(b) = \beta_0. \end{cases}$$

Case 1. Assume that $\alpha(t) = 2t$, $\beta(x) = \frac{1+x}{2}$, $q = 2$, $r = 4$, $\beta_0 = 1$, when $u(t) = t^2$, $f(t) = \frac{\Gamma(3)t^{2-\alpha(t)}}{\Gamma(3-\alpha(t))} + q\frac{\Gamma(3)t^{2-\beta(t)}}{\Gamma(3-\beta(t))} + 4t^2$.

Case 2. (Constant-fractional-order example): Suppose that $\alpha(t) = 2$, $\beta(t) = \frac{1}{2}$, $q = 1$, $r = 1$, when $u(t) = t^2$, $f(t) = t^2 + 2 + \frac{2.666666667t^{1.5}}{\Gamma(0.5)}$.

The maximum absolute errors for Case 1 and Case 2 under different values of n are presented in Tables 3 and 4, respectively, along with comparisons to existing results from Refs. [4, 19].

Table 3 also discusses the CPU for different n. In Table 4, e denotes the absolute error reported in Ref. [19], while e_2 and e_3 correspond to the errors of Method 2 and Method 3 in Ref. [4], respectively. Additionally, Table 5 lists the pointwise errors for both cases with varying n. The absolute error distributions for Case 1 and Case 2 are further illustrated in Figures 1 and 2, respectively.These two figures illustrate that the proposed method can yield excellent results for a variety of fractional differential equations with multiple variables.

Table 3. The maximum absolute errors of Example 5.2, Case 1.

n	2	3	4	5
ME_n in [19]	5.7506e–16	8.88178e–16	5.66214e-15	9.82547e–15
ME_n our method	2.1403e–16	3.90304e–16	2.9530e–16	2.32358e–16
CPU	0.0468	0.125	0.2187	0.3593

Table 4. The maximum absolute errors of Example 5.2, Case 2.

n	e in [19]	e_2 in [4]	e_3 in [38]	our method $n = 3$	our method $n = 4$
ME_n	5.22515e–11	4.30e–05	7.00e-5	1.58e–11	1.58e–11

Table 5. The absolute errors of Example 5.2.

x	Case 1 $(n = 3)$	Case 1 $(n = 4)$	Case 2 $(n = 3)$	Case 2 $(n = 4)$
0.1	8.968e–19	4.259e–18	4.341e–14	4.123e–14
0.2	4.646e–18	1.725e–17	1.136e–13	1.112e–13
0.3	2.406e–17	3.884e–17	9.731e–14	9.798e–14
0.4	5.938e–17	6.833e–17	1.454e–13	1.414e–13
0.5	1.086e–16	1.043e–16	7.740e–13	7.693e–13
0.6	1.671e–16	1.450e–16	1.961e–12	1.958e–12
0.7	2.291e–16	1.879e–16	3.886e–12	3.887e–12
0.8	2.891e–16	2.298e–16	6.730e–12	6.732e–12
0.9	3.431e–16	2.670e–16	1.066e–11	1.066e–11

Example 5.3. Consider the multi-term variable fractional problem:

$$\begin{cases} D_0^{\alpha(t)}u(t) + q_1(t)D_0^{\beta_1(t)}u(t) + q_2(t)D_0^{\beta_2(t)}u(t) + q_3(t)D_0^{\beta_3(t)}u(t) + r(t) * u(t) = f(t), & t \in (0,2), \\ u(0) = 0, u(2) = \dfrac{5}{2}. \end{cases}$$

With $p = 1$, $q_1(x) = t^{\frac{1}{2}}$, $q_2(t) = t^{\frac{1}{3}}$, $q_3(t) = t^{\frac{1}{4}}$, $r(t) = t^{\frac{1}{5}}$. And $\alpha(t) = \frac{t}{5}$, $\beta_1 = \frac{1}{10}$, $\beta_2 = \frac{3}{5}$, $\beta_1 = \frac{4}{5}$. If $u(t) = \frac{5t^3}{2}$, $f(x) = \frac{5\Gamma(4)}{2}(\frac{t^{3-\alpha(t)}}{\Gamma(4-\alpha(t))} + q_1(t)\frac{t^{3-\beta_1}}{\Gamma(4-\beta_1)} + q_2(t)\frac{t^{3-\beta_2}}{\Gamma(4-beta_2)} + q_3(t)\frac{t^{3-\beta_3}}{\Gamma(4-\beta_3)}) + r(t)\frac{5t^3}{2}$.

Figure 3 presents the exact and the approximate solutions for Example 5.3 for $n = 4$. As expected, the numerical results are the same as the exact solution. Figure 4 is the absolute error of Example 5.3 for $n = 5$.

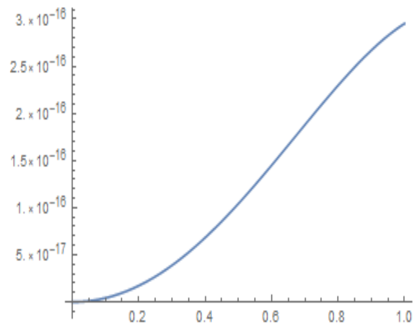

Figure 1. The absolute error of Example 5.2 for Case 1.

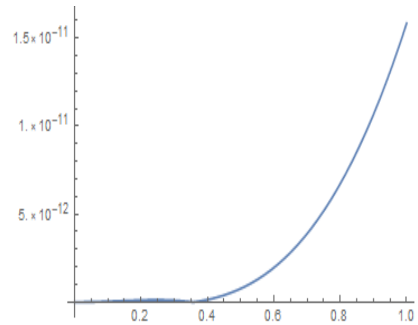

Figure 2. The absolute error of Example 5.2 for Case 2.

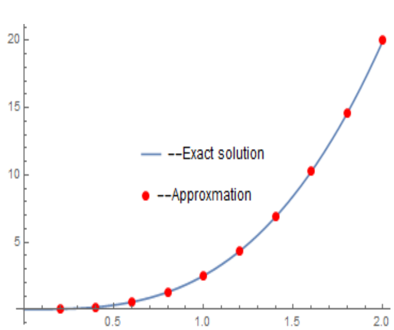

Figure 3. The exact and approximate solutions for Example 5.3.

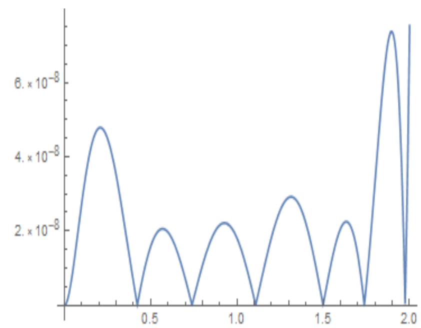

Figure 4. The absolute error of Example 5.3.

Example 5.4. Consider the multi-term variable fractional problem with weak singularity at $t = 0$:

$$\begin{cases} D^{\alpha(t)}u(t) + a(t)D^{\beta(t)}u(t) + q(t) * u(t) = f(t), \quad t \in (0,1), \\ u(0) = 0, \ u(1) = 0. \end{cases}$$

With $\alpha(t) = \frac{1+\sin t}{2}$, $\beta(t) = \frac{2+t}{4}$, $a(t) = t^{0.3}$, $q(t) = t^{0.2}$. Assume $u(t) = t^{\mu}$, where the value of $f(t)$ depends on the choice of μ. From Table 6, it can be observed that the absolute error varies with different values of μ and n. It is evident that when $\mu = 2$, the solution is non-singular at $t = 0$, and the absolute error achieved is the best. According to Figures 5 and 6, it can be seen that the primary reason for the poor absolute error in the other cases is the singularity at $t = 0$.

Table 6. The maximum absolute errors of Example 5.4 for different μ and n.

μ	μ=0.8	μ=1.3	μ=1.5	μ=1.8	μ=2
ME_5	5.82e–02	8.70e–03	3.53e–03	5.80e–04	1.43e–14
ME_6	4.74e–02	6.24e–03	2.40e–03	3.65e–04	1.01e–14

Example 5.5. (Transverse vibration of a viscoelastic rod with variable-order damping) Consider the single-mode approximation of a fixed-fixed viscoelastic rod subjected to a harmonic transverse excitation. This problem models the dynamic behavior of soft materials with time-

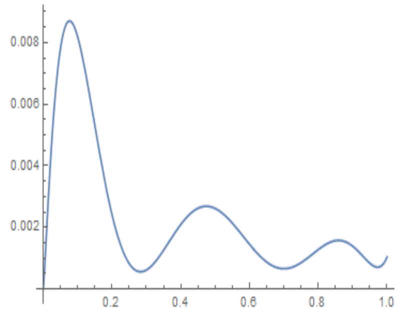

Figure 5. The absolute error of Example 5.4 ($\mu = 1.3$, $n = 5$).

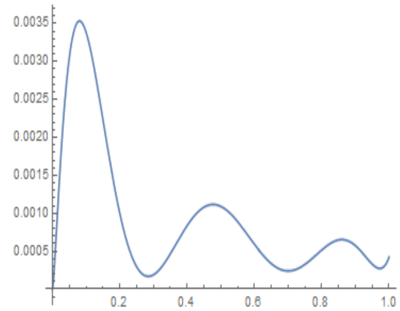

Figure 6. The absolute error of Example 5.4 ($\mu = 1.8$, $n = 5$).

dependent viscoelastic properties, which can be described by the following multi-term variable-order fractional differential equation:

$$\begin{cases} D^{\alpha(t)}u(t) + a(t)D^{\beta(t)}u(t) + k_1 u(t) = F(t), \quad t \in (0,5), \\ u(0) = 0, u'(0) = 0. \end{cases}$$

The variable order is taken as $\alpha(t) = 1.2 + 0.1\sin(x)$ and $\beta(t) = 0.8$. The damping coefficient is $a(t) = 0.1$, the natural frequency is $k_1 = (\pi)^2$ and the external forcing is $F(t) = \sin(2\pi t)$. This problem has no known exact solution due to the variable-order term. To validate the proposed method, we examine the residual convergence and perform a grid refinement analysis. The numerical results demonstrate the effectiveness of our Legendre polynomial-based approach in capturing the complex dynamic behavior of viscoelastic structures with time-varying material properties.

The residual in this paper is defined as follows

$$R_n(t) = D^{\alpha(t)}u(t) + a(t)D^{\beta(t)}u(t) + k_1 u(t) - F(t).$$

The residual norm is $Res_n = \|R_n(t)\|_{L^2}$. Table 7 shows that Res_n gradually approaches 0 as n increases. Figures 7 and 8 illustrate $u_n(t)$ when n=4 and n=8, respectively.

Table 7. The residual norm Res_n of Example 5.5 for different n.

n	4	5	6	7	8
ME_5	1.50e–01	9.39e–02	7.20e–03	2.35e–03	3.98e–04

In this paper, the grid refinement analysis is employed, taking $n = 4, 5, 6, 7, 8, 9$ to calculate the differences between adjacent similar solutions: $E_n = |u_{n+1} - u_n|$. Table 8 shows that E_n decreases monotonically as n increases.

Table 8. The network convergence analysis of Example 5.5 for different n.

n	4	5	6	7	8
ME_5	2.25e–02	2.40e–02	5.01e–03	2.72e–03	2.27e–04

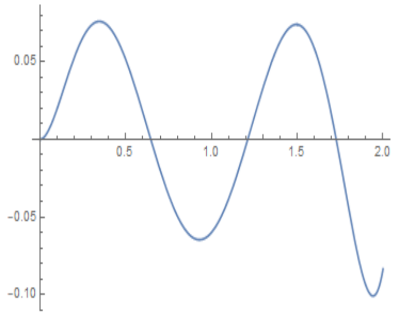

Figure 7. $u_4(t)$ of Example 5.5.

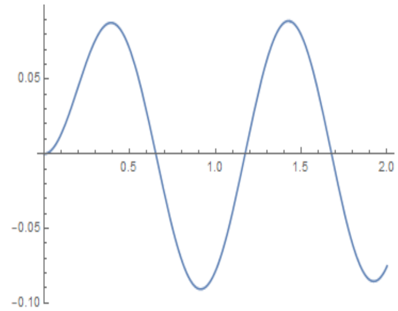

Figure 8. $u_8(t)$ of Example 5.5.

6. Conclusion

This work introduces a high-precision numerical framework for solving multi-term variable-order fractional differential equations. The core idea is to employ Legendre polynomials to construct an orthonormal basis within a reproducing kernel Hilbert space, which facilitates the efficient approximation of solutions with variable fractional orders. Theoretically, we provide a rigorous convergence analysis that guarantees the reliability of the proposed method. Numerically, extensive experiments are carried out to evaluate its performance. Comparative results with existing techniques, detailed in the tables, consistently demonstrate the superior accuracy of our approach. In summary, the proposed algorithm offers a robust and efficient tool for tackling complex fractional differential problems, with potential extensions to other classes of functional equations.

Data availability statement. Data sharing not applicable to this article as no datasets were generated or analyzed during the current study.

Author contributions. Xu proposed research questions and wrote manuscripts. Zhang proposes the method and performed numerical calculations. All authors participated in the writing and revision of the manuscript. All authors read and approved the final manuscript.

Competing interests. The authors have no conflicts of interest to declare that are relevant to the content of this article.

References

[1] C. G. Canuto, M. Y. Hussaini, A. Quarteroni, et al., *Spectral Methods: Fundamentals in Single Domains*, Springer Publishers, 2006.

[2] C. F. M. Coimbra, *Mechanics with variable-order differential operators*, Ann. Phys., 2003, 12, 692–703.

[3] M. Dehghan and M. Safarpoor, *The dual reciprocity boundary integral equation technique to solve a class of the linear and nonlinear fractional partial differential equations*, Math. Meth. Appl. Sci., 2016, 39, 2461–2476.

[4] N. J. Ford and J. A. Connolly, *Systems-based decomposition schemes for the approximate solution of multiterm fractional differential equations*, J. Comput. Appl. Math., 2009, 229, 382–391.

[5] R. M. Ganji and H. Jafari, *A numerical approach for multi-variable orders differential equations using Jacobi polynomials*, Int. J. Appl. Comput. Math., 2019, 5, 34.

[6] R. M. Ganji, H. Jafari and D. Baleanu, *A new approach for solving multi variable orders differential equations with Mittag-Lefflfler kernel*, Chaos, Solitons Fractals, 2020, 130, 109405.

[7] B. Ghanbari and J. F. Gomez-Aguilar, *Modeling the dynamics of nutrient-phytoplankton-zooplankton system with variable-order fractional derivatives*, Chaos, Solitons and Fractals, 2018, 116, 114–120.

[8] K. A. Hassan and M. Dehghan, *The sine and cosine diffusive representations for the Caputo fractional derivative*, Annals of Nuclear Energy, 2022, 166, 108709.

[9] E. Hesameddini, A. Rahimi and E. Asadollahifard, *On the convergence of a new reliable algorithm for solving multi-order fractional differential equations*, Commun. Nonlinear Sci. Numer. Simul., 2016, 34, 154–164.

[10] Y. T. Jia, M. Q. Xu and Y. Z. Lin, *A numerical solution for variable order fractional functional differential equation*, Appl. Math. Lett., 2017, 64, 125–130.

[11] Y. Jia, M. Xu, Y. Lin and D. Jiang, *An efficient technique based on least–squares method for fractional integro-differential equations*, Alex. Eng. J., 2023, 64, 97–105.

[12] B. Jin, R. Lazarov, Y. Liu and Z. Zhou, *The Galerkin fifinite element method for a multi-term time-fractional diffusion equation*, J. Comput. Phys., 2015, 281, 825–843.

[13] A. A. Kilbas, H. M. Srivastava and J. J. Trujillo, *Theory and Applications of Fractional Differential Equations*, Elsevier: North-Holland Mathematics Studies, 2006.

[14] X. Li and B. Wu, *A numerical technique for variable fractional functional boundary value problems*, Appl. Math. Lett., 2015, 43, 108–113.

[15] F. Liu, P. Zhuang and Q. Liu, *Numerical methods of fractional partial differential equations and applications*, Beijing: Science Press, 2015.

[16] A. Lotfi, S. A. Yousefi and M. Dehghanb, *Numerical solution of a class of fractional optimal control problems via the Legendre orthonormal basis combined with the operational matrix and the Gauss quadrature rule*, J. Comput. Appl. Math., 2013, 250, 143–160.

[17] Z. M. Mohamed, Y. Mohammed and E. H. Amjad, *Solving nonlinear fractional partial differential equations using the elzaki transform method and the homotopy perturbation method*, Abstr. Appl. Anal., 2022, 1–9. https://doi.org/10.1155/2022/4743234.

[18] K.-H. Pho, M. H. Heydari, B. A. Tuan and M. R. Mahmoudid, *Numerical study of nonlinear 2D optimal control problems with multi-term variable-order fractional derivatives in the Atangana-Baleanu Caputo sense*, Chaos Solitons Fractals, 2020, 13, 109695.

[19] S. N. T. Polat and A. T. Dincel, *Numerical solution method for multi-term variable order fractional differential equations by shifted Chebyshev polynomials of the third kind*, Alex. Eng. J., 2022, 61, 5145–5153.

[20] P. Roul, *A robust adaptive moving mesh technique for a time-fractional reaction-diffusion model*, Commun. Nonlinear Sci. Numer. Simul., 2022, 109, 106290.

[21] P. Roul and V. Rohil, *A high order numerical technique and its analysis for nonlinear generalized Fisher's equation*, J. Comput. Appl. Math., 2022, 406, 114047.

[22] P. Roul and V. Rohil, *A high-order numerical scheme based on graded mesh and its analysis for the two-dimensional time-fractional convection-diffusion equation*, Comput. Math. Appl., 2022, 126, 1–13.

[23] P. Roul and V. Rohil, *A novel high-order numerical scheme and its analysis for the two-dimensional time-fractional reaction-subdiffusion equation*, Numer. Algorithms, 2022, 90, 1357–1387.

[24] P. Roul, V. Rohil, et. al., *Numerical simulation of two-dimensional fractional neutron diffusion model describing dynamical behaviour of sodium-cooled fast reactor*, Ann. Nucl. Energy., 2022, 166, 108709.

[25] P. Roul and S. Sundar, *Novel numerical methods based on graded, adaptive and uniform meshes for a time-fractional advection-diffusion equation subjected to weakly singular Solution*, Numer. Algorithms, 2015, 98, 531–561.

[26] Y. Wang, L. Zhu and Z. Wang, *Solving the nonlinear variable order fractional differential equations by using euler wavelets*, CMES, 2019, 118, 339–350.

[27] B. Wu and Y. Lin, *Application of the reproducing kernel space*, Beijing: Science Press, 2012.

[28] M. Xu, E. Tohidi, J. Niu and Y. Fang, *A new reproducing kernel-based collocation method with optimal convergence rate for some classes of BVPs*, Appl. Math. Comput., 2022, 432, 127343.

[29] M. Xu, L. Zhang and E. Tohidi, *A fourth-order least-squares based reproducing kernel method for one-dimensional elliptic interface problems*, Appl. Numer. Math., 2021, 162, 124–136.

[30] M. Xu, L. Zhang and E. Tohidi, *An efficient method based on least–squares technique for interface problems*, Appl. Math. Lett., 2023, 136, 108475.

[31] S. S. Zeid, H. Jahanshahi, A. Yousefpour, et al., *King algorithm: A novel optimization approach based on variable-order fractional calculus with application in chaotic financial systems*, Chaos, Solitons and Fractals, 2020, 132, 109569.

[32] P. Zhang, Y. C. Zhang, Y. T. Jia and Y. Z. Lin, *A novel algorithm for time fractional advection-diffusion equation*, Math Method Appl. Sci., 2025, 9(48), 10082–10095.

[33] Q. Zhang, Y. L. Shang, Y. Li, et al., *A novelfractional variable-order equivalent circuit model and parameter identification of electric vehicle li-ion batteries*, ISA Transactions, 2020, 97, 448–457.

[34] Y. C. Zhang, Y. T. Jia and Y. Z. Lin, *An $\varepsilon-$approximate solution of BVPs based on improved multiscale orthonormal basis*, AIMS. Math., 2024, 9(3), 5810–5826.

[35] Y. C. Zhang and Y. Z. Lin, *A $\varepsilon-$approximation solution of time–fractional diffusion equations based on Legendre polynomials*, AIMS. Math., 2024, 9(6), 16773–16789.

[36] Y. C. Zhang, L. C. Mei and Y. Z. Lin, *A new method for high-order boundary value problems*, Bound. Value Probl., 2021, 48, 1–13.

[37] Y. C. Zhang, L. C. Mei and Y. Z. Lin, *A novel method for nonlinear boundary value problems based on multiscale orthogonal base*, Int. J. Comp. Meth., 2021, 18(09), 2150036.

[38] Y. C. Zhang, H. B. Sun, Y. T. Jia and Y. Z. Lin, *An algorithm of the boundary value problem based on multiscale orthogonal compact base*, Appl. Math. Lett., 2020, 101, 106044.

Received November 2025; Accepted June 2026; Available online June 2026.